

HIGHLY PRECISE CORRELATION ESTIMATES OF TURBULENT SHEER FLOWS USING A NOVEL LASER DOPPLER PROFILE SENSOR

Mathias Neumann, Katsuaki Shirai, Andreas Voigt, Lars Büttner, Jürgen Czarske
Chair of Measurements and Test Techniques,
TU Dresden
01062 Dresden, Germany
mathias.neumann@tu-dresden.de

ABSTRACT

For the characterisation of small vortices within turbulent flow fields the Taylor length scale is often used. This length scale can be extrapolated out of two-point correlation estimations for which the flow velocity has to be measured precisely at two different positions in the flow. The application of the laser Doppler velocity profile sensor, which offers a high spatial resolution within the measurement volume (around 10 μm) and a low velocity measurement uncertainty of about 0.1 %, for vortex investigations is, therefore, an interesting novel approach. Moreover, the system offers the advantage of extrapolating the Taylor length scale with data from only one sensor which is not possible with conventional laser Doppler velocimetry. Due to the high spatial resolution of profile sensor, problems which occur when the detection volumes overlap do not occur in contrast to conventional systems. We present measurements which have been carried out in the turbulent wake of a circular cylinder. Both temporal as well as spatial correlation estimations have been calculated out of the acquired velocity data.

INTRODUCTION

The investigation of turbulence structures consisting of small eddies, appearing e.g. behind obstacles in turbulent flows, allows clarifying the fundamental characteristics of the flow itself. One specific scale for describing a certain size of eddies is the Taylor length scale. In order to determine this length scale, spatial or, under the assumption of a locally isotropic flow, temporal correlation estimations have to be performed and finally, the Taylor length scale can be extrapolated out of these data. Consequently, highly precise velocity measurements have to be performed simultaneously at different positions within the flow field. Up to now, different techniques like particle image velocimetry (PIV), conventional laser Doppler velocimetry (LDV) or hot-wire anemometry (HWA) have already been applied for such kind of measurements. Nevertheless, these techniques do suffer from drawbacks like moderate spatial resolution (around 100 μm) or intolerable velocity measurement uncertainties (PIV ca. 3%), whereas systems like HWA are intrusive and, therefore, disturb the flow. For measuring the stream velocity at different, exactly determined positions simultaneously, two measurement volumes/probes are necessary in case of LDV or HWA measurement setups (Fraser et al., 1986, Trimis and Melling, 1995). This may cause uncertainties due to imprecise positioning and averaging. The laser Doppler velocity profile sensor is a novel measurement technique for correlation estimations which will be presented hereafter. With its high spatial resolution within the measurement volume and the low velocity measurement uncertainty, the profile sensor is ideal for correlation esti-

mations. It offers the opportunity of quasi simultaneously measuring velocities at different positions without traversing the sensor or applying a second measurement volume. Moreover, with the novel developed signal processing software, a data rate of more than 1.5 kHz could be achieved which is mandatory for correlation estimations.

LASER DOPPLER VELOCITY PROFILE SENSOR

The laser Doppler velocity profile sensor, which can be considered as an extended LDV system, forms two physically distinguishable, overlapping fan-like fringe systems in the measurement volume. In contrast to conventional LDV, the fringe spacing is not kept constant within the measurement volume but one diverging and one converging fringe system is applied (Czarske, 2002). A seeding particle passing the measurement volume emits scattered light which exhibits a Doppler frequency shift. Due to the two fringe systems, a tracer particle generates two Doppler frequencies $f_{1,2}$ which can be used to determine both, the velocity as well as the axial position z where the particle passed fringe system. During the calibration with the velocity u , predetermined by a chopper wheel, the quotient $q(z)$ is calculated out of the two Doppler frequencies f_1 and f_2 as follows:

$$q(z) = \frac{f_2(u, z)}{f_1(u, z)} = \frac{u(z)/d_2(z)}{u(z)/d_1(z)} = \frac{d_1(z)}{d_2(z)}. \quad (1)$$

With the known velocity during the calibration the fringe spacing follows as:

$$d_i(z) = \frac{u}{f_i(u, z)}. \quad (2)$$

The velocity u of a particle can be calculated in general with the help of the known fringe spacing d_i ($i=1, 2$) with:

$$u = f_1(u, z) \cdot d_1(z) = f_2(u, z) \cdot d_2(z). \quad (3)$$

The obtained calibration function $q(z)$ can, thereafter, be used to determine the position z where a particle passed the measurement volume by dividing the two measured Doppler frequencies $f_{1,2}$. With the known fringe spacing at this position, the particle velocity u can finally be calculated. The principle is depicted in figure 1. For the measurements presented here, a sensor setup applying a frequency division multiplexing (FDM) technique has been used (Shirai et al., 2006). The working distance of the system is 56 cm and the measurement volume has a longitudinal extension of about 1600 μm . For future measurements, a setup with a smaller measurement volume is planned.

DATA ACQUISITION AND PROCESSING

Since the measurement principle of the profile sensor bases on the Doppler frequency shift, the precision and speed

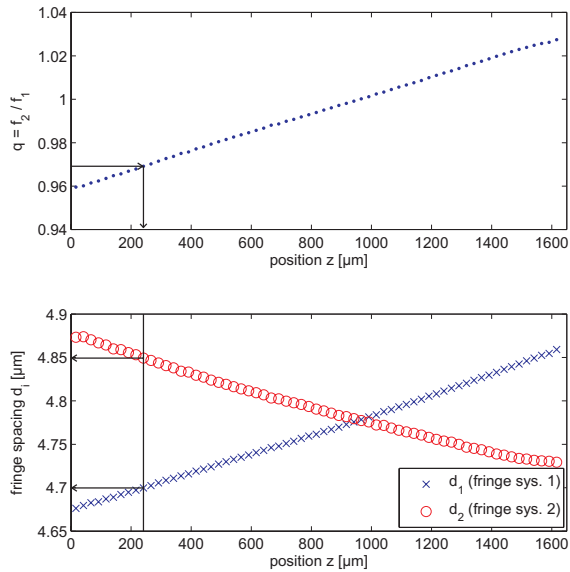


Figure 1: Determination of position and velocity of a particle within the measurement volume.

of the signal processing software plays an important role for the measurement uncertainty. The evaluation of the Doppler frequency of the tracer particles leads to their velocity which, under the assumption of slip free movement, represents the flow velocity. The scattered light is detected by an avalanche photodetector (APD) which converts the light intensity into an electrical signal which is then captured by an A/D converter card installed in a standard computer. The signal evaluation is performed by a combined Matlab and C programme which offers high flexibility and is adapted to the profile sensor. Moreover, all detected burst signal are recorded including a timestamp which is necessary for the correlation calculations (see section “CORRELATION ESTIMATIONS”). The frequency of the burst signal is calculated using the quadrature demodulation technique (QDT) which is explained shortly in the following. In general, a time signal of a burst can be described as follows (discrete notation):

$$m(t_k) = A \cdot e^{-n(t_k - T)^2} \cdot \cos(2\pi f_d \cdot t_k + \varphi) \quad (4)$$

with: A ...amplitude; f_s ...sampling frequency
 n ...width of the burst; f_d ...Doppler frequency
 T ...occurrence time; φ ...phase
 t_k ...discrete sampling time ($t_k = k/f_s, k \in \mathbb{N}^+$).

Hence, the Fourier transform $M(f_g) = \mathcal{F}\{m(t_k)\}(f_g)$ of such a burst signal reads:

$$M(f_g) = \frac{A \cdot f_s}{2} \sqrt{\frac{\pi}{n}} \cdot e^{-\frac{\pi^2}{n}(f_d - f_g)^2 + j(2\pi(f_d - f_g)T + \varphi)}. \quad (5)$$

After removing the constant component, the Doppler frequency f_d can be roughly estimated as the frequency belonging to the maximum peak in the spectrum. After the inverse Fourier transform of the half sided spectrum the analytical signal follows as:

$$m_a(t_k) = m(t_k) + j \cdot m_H(t_k) \quad (6)$$

with: $m_H(t_k)$...Hilbert transform ($\mathcal{H}\{m(t_k)\}(t_k)$).
 The instantaneous phase ϕ reads as follows:

$$\Phi(t_k) = \arctan \frac{m_H(t_k)}{m(t_k)}. \quad (7)$$

Finally, the Doppler frequency f_d can be evaluated by averaging the instantaneous frequency as follows (Bayer et al., 2008):

$$f_d = \frac{\overline{\omega}}{2\pi} = \frac{1}{2\pi} \cdot \overline{\left(\frac{d\Phi}{dt}\right)}. \quad (8)$$

For the experiments undertaken, velocities of about 10 m/s had to be measured and the ellipsoidal measurement volume does have a diameter of circa 180 μm . This results in a mean residence time of a particle within the volume of around 18 μs . Furthermore, the particle distribution follows a Poisson statistics and, as a result, the statistics of the time between two detected particles can be described with an exponential distribution. As a result, low interarrival times are the most probable events (Albrecht et al., 2003). Due to the fact of high particle rates which have to be processed, the data acquisition and signal evaluation have to be fast enough. The signal processing software was tested with model burst signals from an arbitrary signal generator. The maximum data rate, i.e. evaluated bursts per second, achieved was 3.25 kHz. The high data rate is mandatory in order to achieve satisfying results for the correlation estimations. This is due to the fact that turbulent flows have high frequency oscillations of typically up to several kHz. Moreover, for spatial correlation estimations it is inevitable to correlate the fluctuating velocity component of two particles which pass the measurement volume at different positions but ideally at the same time (zero lag time). Since the current setup of the laser Doppler velocity profile sensor only applies one detector, the detection of two particles at exactly the same time is difficult since it results in a so called dual-burst signal. Therefore, one of the most important parameters of the signal processing hard- and software is the minimal measurable lag time. During the same test measurements, the smallest detectable interarrival times have been investigated. These could be determined to be lower than 20 μs which is much smaller than the smallest time scale of the flow investigated where it is assumed to be higher than 40 μs (see section “RESULTS”). Comparing the minimum residence time of a particle in the measurement volume, which is around 18 μs , with the minimum measurable lag time the data acquisition hard- and software demonstrated adequate processing speed.

CORRELATION ESTIMATIONS

In the following section, the new opportunities of the profile sensor concerning correlation estimations shall be discussed. The high spatial resolution within the measurement volume offers an advantage compared to conventional LDV systems. In general, the velocity fluctuations u' occurring in the flow which are caused by vortices show specific relations. A measure of these relations is the normalized spatial temporal correlation function $\rho(\Delta z, \tau)$ which reads as follows:

$$\rho(\Delta z, \tau) = \frac{\overline{u'(z, t) \cdot u'(z + \Delta z, t + \tau)}}{\sqrt{\overline{u'(z, t)^2}} \cdot \sqrt{\overline{u'(z + \Delta z, t + \tau)^2}}}. \quad (9)$$

In this equation Δz represents the shift of the two detection volumes with respect to each other. The variable Δt represents the maximum allowed time difference (lag time) between two measured burst signals in each measurement volume. The time difference between the two signals is not allowed to exceed the smallest time scale of the flow. Figure 2 depicts the difference between LDV and profile sensor setups for spatial correlation estimations.

In order to estimate the Taylor length scale, a parabola

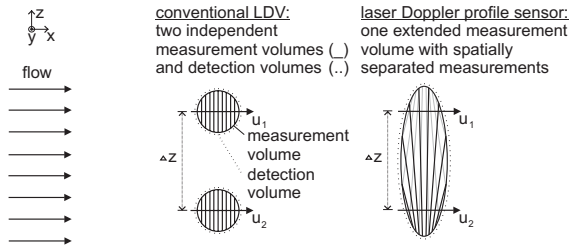


Figure 2: Comparison between conventional LDV and laser Doppler velocity profile sensor.

$h(\Delta z)$ has to be fitted at the values of the correlation function around $\Delta z = 0$. The intersection of the parabola with the axis of abscissae equals the Taylor length scale of the investigated flow.

Another method for calculating the correlation estimation is an indirect one which is only applicable under certain flow conditions. In case of $u' \ll \bar{u}$ (Reynolds decomposition: $u = \bar{u} + u'$) the Taylor hypothesis of frozen flow states that spatial velocity fluctuations appear almost undistorted as temporal fluctuations in case they are convected rapidly through the measurement volume by the mean flow (Pope, 2000). Hence, the dependency follows as:

$$t = \frac{x}{\bar{u}} \Rightarrow \overline{\left(\frac{\partial u}{\partial x}\right)^2} = \frac{1}{\bar{u}^2} \cdot \overline{\left(\frac{\partial u}{\partial t}\right)^2}$$

$$\overline{\left(\frac{\partial u_1}{\partial x_1}\right)^2} = \frac{2 \cdot \overline{u'^2}}{\lambda_f^2}. \quad (10)$$

For temporal correlation estimations, only one measurement volume is applied and the correlation coefficients for different lag times τ are calculated according to equation (9) while keeping $\Delta z = 0$. In this case, a fitted parabola $g(\tau)$ around $\tau = 0$ can be used as well to determine the Taylor length scale λ .

Temporal correlation

The temporal correlation can, in general, be estimated easier since only one measurement volume is necessary. The temporal correlation function equals equation (9) with a fixed $\Delta z = 0$, since the measurement is performed at only one position, and variable τ . Furthermore, the algorithm applies local normalisation (van Maanen and Tummers, 1996) and fuzzy-slotting (Nobach et al., 1998). Moreover, the forward-backward weighting technique (Nobach, 1999) is used to correct τ in order to improve the precision of the correlation estimation. The algorithms read as follows:

$$\rho(k \cdot \tau) = \frac{\sum_{i=1}^N \sum_{j=1}^N u'_i \cdot u'_j \cdot b_k(t_i, t_j)}{\sqrt{\left(\sum_{i=1}^N \sum_{j=1}^N u'^2_i b_k(t_i, t_j)\right) \left(\sum_{i=1}^N \sum_{j=1}^N u'^2_j b_k(t_i, t_j)\right)}}$$

$$\tau_k = \frac{\sum_{i=1}^{N-1} \sum_{j=i+1}^N (t_j - t_i) \cdot w_i \cdot w_j \cdot b_k(t_j, t_i)}{\sum_{i=1}^{N-1} \sum_{j=i+1}^N w_i \cdot w_j \cdot b_k(t_j, t_i)} \quad (11)$$

$$with : b_k(t_i, t_j) = \begin{cases} 1 - \left| \frac{t_j - t_i}{\tau} - k \right| & \text{for } \left| \frac{t_j - t_i}{\tau} - k \right| \leq 1 \\ 0 & \text{else} \end{cases}$$

$$w_i = t_{i+1} - t_i$$

$$w_j = t_j - t_{j-1}.$$

After calculating the temporal correlation estimation, the longitudinal Taylor length scale can be estimated by fitting a parabola as explained above.

Spatial correlation

As mentioned, the LDP offers completely new opportunities concerning the spatial correlation technique. The Taylor length scale can be derived from spatial correlation estimations but, in contrast to temporal correlations, now further assumptions concerning the flow are necessary. The high spatial resolution of the profile sensor makes new processing techniques possible which are described in the following sections.

Virtual detection volumes. In case of spatial correlation estimations, the profile sensor offers the novel opportunity to divide the measurement volume into different detection volumes virtually. Since the profile sensor allows a position determination for each particle detected, the measurement volume can be fragmented during the post processing. The algorithm for the spatial correlation estimation firstly separates the complete measurement volume into multiple, i.e. two, smaller virtual detection volumes (slots) with a defined size l . The virtual slot, which is not moved, is positioned directly at the border of the measurement volume ($z = 0$). The algorithm only processes the data of particles which have passed the measurement volume within the boundaries of the specific slot. The application of virtual detection volumes is depicted in figure 3. The centre c_{var} and the upper and lower bound b_{up} and b_{low} of the variable slot, whose fluctuating velocity values are correlated with the data of the fixed one, is calculated according to the following equations:

$$c_{var}(k) = \Delta z = k \cdot dz = k \cdot \frac{l}{m}; \quad (k \in \mathbb{N}, m \in \mathbb{R})$$

$$b_{up} = c_{var} + \frac{l}{2} = \left(\frac{k}{m} + \frac{1}{2}\right) \cdot l \quad (12)$$

$$b_{low} = c_{var} - \frac{l}{2} = \left(\frac{k}{m} - \frac{1}{2}\right) \cdot l.$$

As shown, the algorithm always shifts the variable slot by a constant value dz , usually half of the slot size. Nevertheless, parameters like slot size l and shifting distance dz can be adjusted flexibly. The size of the virtual detection volumes is a critical issue. In contrast to increased spatial resolution of the correlation function when selecting slots as small as possible, the amount of detected burst signals within one slot decreases. Since also the maximum allowed lag time has to be considered, a trade-off has to be found. This can be overcome by simply measuring longer but is definitely a critical aspect, especially considering the dual-burst problem. Another advantage offered by the profile sensor is the potential to distinguish self-products when calculating slots which are overlapping. This is not possible when using conventional setups and offers an opportunity to improve the correlation estimation even more in the region where it is needed, i.e. where the function is fitted.

Spatial temporal correlation. The axial positional resolu-

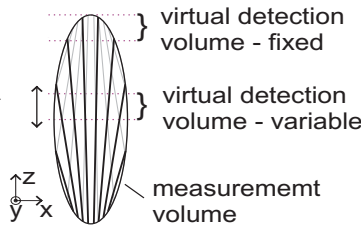


Figure 3: Principle of virtual detection volumes.

tion of two independent particles for the profile sensor can be increased to nearly the physical size of the tracer particles inside the measurement volume. Hence, a sufficient spatial resolution can be achieved to resolve the Taylor length scale while keeping the data rate high and without necessitating the side scatter detection for the lateral positional information of particles inside the measurement volume. One challenge which arises from the profile sensor is the evaluation of two particles which pass the measurement volume at almost the same time. As described in section “DATA ACQUISITION AND PROCESSING”, particles with interarrival times down to 20 μs could be measured at data rates larger than 3 kHz and the effect can, therefore, be tolerated. Moreover, also conventional LDV correlation setups suffer from a low number of particles passing the two measurement volumes at the same time. One solution is to apply a spatial time correlation. This method allows a certain lag time between two passing particles which has to be selected smaller than the smallest timescale (Kolmogorov time scale) within the turbulent motion. The algorithm, which is derived from equation (9) reads as follows:

$$\rho(\Delta z, \tau) = \frac{\sum_{i=1}^N \sum_{j=1}^N u'_i(0) \cdot u'_j(\Delta z) \cdot b_k(t_i, t_j)}{\sqrt{\left(\sum_{i=1}^N \sum_{j=1}^N u'^2_i(0) b_k(t_i, t_j) \right) \left(\sum_{i=1}^N \sum_{j=1}^N u'^2_j(\Delta z) b_k(t_i, t_j) \right)}} \quad (13)$$

$$\text{with: } b_k(t_i, t_j) = \begin{cases} 1 & \text{for } \left| \frac{t_j - t_i}{\tau} \right| \leq 1 \\ 0 & \text{else.} \end{cases}$$

With the setup shown in figure 3, the correlation function perpendicular to the main flow direction can be calculated and the transverse Taylor length scale can be evaluated.

MEASUREMENT SETUP

Measurements have been carried out in the wake of a circular cylinder. The experimental setup has been chosen analogue to Absil et al. (1990) with a difference in the mean velocity which was measured to be $\bar{u} = 9.1$ m/s. The reason of the lower mean velocity, compared to Absil’s experiment (10 m/s), is the setup of the existing wind tunnel which could not achieve higher velocities. Nevertheless, the achievable results should show the tendencies and lie within the same range so that the results allow a comparison in terms of plausibility. A stainless-steel circular cylinder (diameter $d=2$ mm) was mounted directly in front of the nozzle of the open loop wind tunnel. The resulting Reynolds’ number was $Re=1200$ and the Strouhal-number was estimated as 0.2. Therefore, the vortex frequency follows as 956 Hz. The smallest time scale of the flow is expected to be higher than 40 μs. This time scale data has been investigated by Absil et

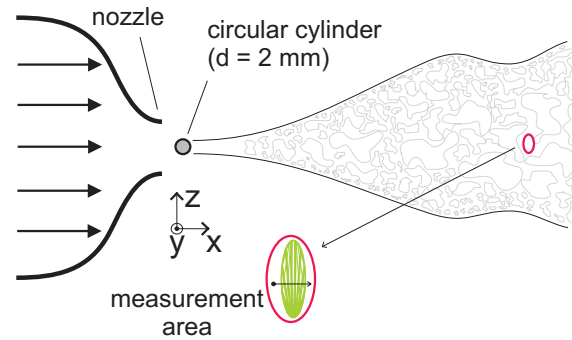


Figure 4: Measurement setup.

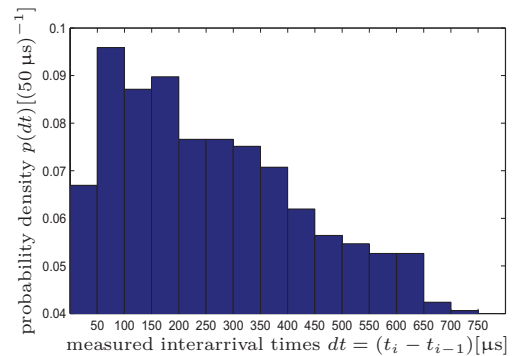


Figure 5: Discrete probability density of interarrival time.

al. and since our measurement conditions differ, i.e. lower mean velocity u yielding a lower degree of turbulence, the smallest time scale of the flow should be a little bit larger than estimated by Absil et al. Measurements have been performed in the turbulent wake of the cylinder 25 cm downstream ($x/d=125$). DEHS (di-ethylhexyl-sebacate) with a mean particle size of one micron was used to create a dense seeding in order to achieve high data rates. The setup is depicted in figure 4.

During the measurements, the mean SNR was determined to 5.1 dB which is caused by the low SNR acceptance level set at the signal processing algorithm. As described in Bayer et al. (2008) the resulting position measurement uncertainty σ_{z0} can be calculated as follows:

$$\sigma_{z0} = \delta_{z0} \cdot \frac{d_0}{c} = 0.0004 \cdot \frac{4.779 \mu\text{m}}{10^{-4}} = 19.1 \mu\text{m} \quad (14)$$

with: δ_{z0} ...normalized uncertainty

d_0 ...fringe spacing at centre of measurement volume

c ...mean slope of calibration curve (dq/dz).

The recorded dataset for each measured particle consists of the velocity u in x-direction, the passing position z within the measurement volume and the arrival-time $t_{arrival}$.

RESULTS

During the measurement more than 1.5 million datasets (axial position, lateral velocity component and arrival time) have been recorded. For the purpose of proving the ability of the measurement system, the statistics about the measured particle interarrival times has been calculated (see figure 5). The lowest measured interarrival times were below 24 μs. Compared to the demonstrated results in the benchmark tests, the measurement system was able to perform equally well during the flow measurements. Nevertheless, the low

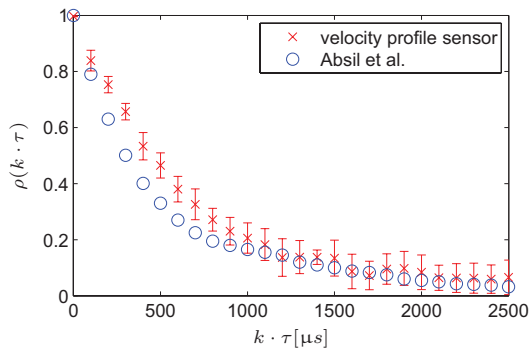


Figure 6: Temporal correlation estimation comparison.

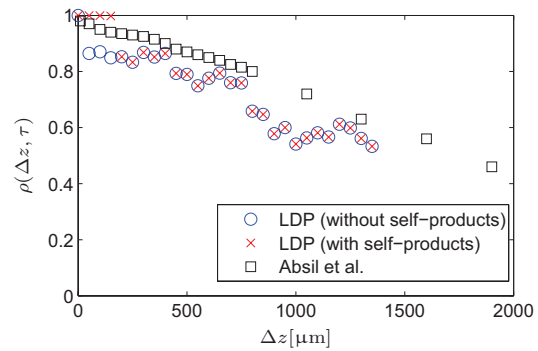


Figure 8: Spatial time correlation result comparison.

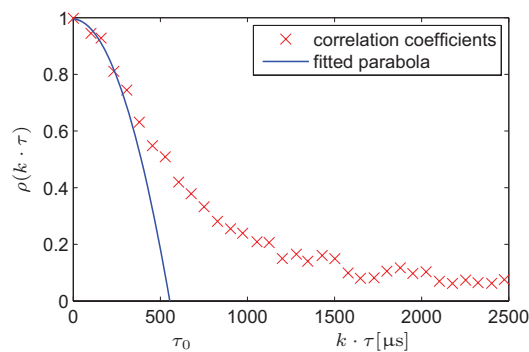


Figure 7: Temporal correlation estimation with lag time weighting and fitted parabola.

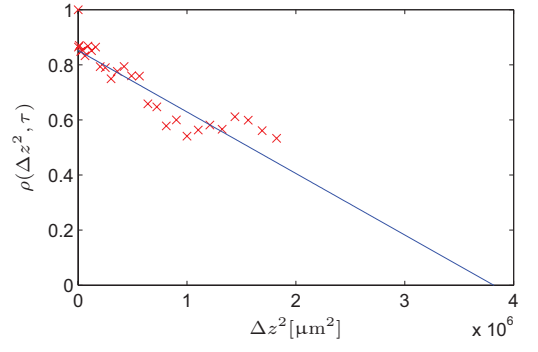


Figure 9: Spatial correlation with fitted function.

interarrival times ($dt \leq 50 \mu s$) are underrepresented, assuming an exponential interarrival time statistics. This is due to the fact that occurring dual-burst signals have not been evaluated. This also shows the necessity of further expanding the evaluation algorithm for the next measurements in order to be able to evaluate such signals. The mean validated data rate was approximately 1.5 kHz. One reason for the data rate is the density of the seeding which could not be increased further in the existing wind tunnel.

Temporal correlation results

The measurement data consisted of consecutive record sets, taken at $z/d=0$, with around 7,500 evaluated bursts per set. This length of each record set was limited by the memory of the data acquisition card. For each record set the temporal correlation has been calculated according to equation (11) (without local time estimation for comparison) and at the end, the averaged correlation coefficients including the statistical standard deviation have been calculated. These data is plotted in comparison to the correlation coefficients estimated by Absil et al. (1990) in figure 6.

In order to be able to estimate the Taylor length scale a parabola has been fitted to the calculated correlation coefficients for which the local time estimation has been applied for higher accuracy of the estimation. Moreover, the correlation estimation has been corrected using a scheme presented by Nobach (2002). From the final result depicted in figure 7 the longitudinal Taylor length scale follows as:

$$\tau_0 = 550 \mu s = \frac{\sqrt{2}\lambda_f}{\bar{u}} \Leftrightarrow \lambda_f = \frac{550 \mu s \cdot 9.1 m/s}{\sqrt{2}} = 3.53 \text{ mm.} \tag{15}$$

Spatial correlation results

Since the laser Doppler velocity profile sensor is able to determine the axial position within the measurement volume, this can be divided virtually into detection volumes as if two detectors would have been used. A slot size of $200 \mu m$ and a maximum lag time $\tau = 50 \mu s$ has been selected and the correlation coefficients have been calculated. The results are depicted and compared to the ones from Absil et al. (1990) in figure 8. The effect of overlapping at the first four coefficients is visible when the self-products are included.

In order to extrapolate the Taylor length scale, Belmabrouk et al. (1998) suggested fitting a linear function $h(\Delta z^2)$ in a least-square sense to the coefficients of the correlation function $\rho(\Delta z, \tau)$ versus traversing distance Δz squared. The Taylor length scale should be calculated based on fits for different ranges of the shifting distance $\Delta z_{min} - \Delta z_{max}$ followed by the determination of the mean value of the different results. This technique has been applied and figure 9 depicts the correlation coefficients with the fitted linear function $h(\Delta z^2)$ which is used to extrapolate the transverse Taylor length scale λ_g as follows:

$$h(\Delta z_0^2) = 0 \Leftrightarrow \lambda_g = \sqrt{\Delta z_0^2}. \tag{16}$$

For the calculation if the Taylor length scale, $\Delta z_{min} = 200 \mu m$ has been chosen the value for Δz_{max} has been varied. The results of the calculations are shown in table 1 and yield a mean transverse Taylor length scale of $\bar{\lambda}_g \approx 1.84 \text{ mm}$. This is in good agreement with the result of Absil et al. (1990) who determined the Taylor length scale to 1.9 mm.

To conclude, it could be demonstrated for the first time that the laser Doppler velocity profile sensor can be applied to estimate spatial correlation functions without any physical traversing. Moreover, particles occurring in both detection volumes can be identified and discarded for the

Table 1: Taylor length scale λ_g for different ranges of Δz_{max} .

Δz_{min} [μm]	Δz_{max} [μm]	λ_g [μm]	$\frac{ \lambda_g - \lambda_g }{\lambda_g}$
200	450	2092.2	0.122
200	500	1832.8	0.001
200	550	1621.2	0.132
200	600	1701.7	0.078
200	650	1883.0	0.025
200	700	1931.8	0.050
200	750	2012.5	0.088
200	800	1844.5	0.005
200	850	1781.9	0.029
200	900	1692.8	0.084
200	950	1692.7	0.084
200	1000	1668.5	0.099
200	1050	1691.8	0.084
200	1100	1742.0	0.054
200	1150	1789.7	0.025
200	1200	1874.9	0.021
200	1250	1953.7	0.061
200	1300	2009.3	0.087
200	1350	2051.7	0.106
$\lambda_g = 1835 \mu\text{m}$			

correlation estimation which is also not possible with conventional LDV setups.

SUMMARY AND OUTLOOK

We demonstrated a completely new method to determine spatial correlation estimations with a novel laser Doppler velocity profile sensor which does not need traversing. The sensor consists of two fan-like fringe systems which allow a determination of the axial position of particles passing the measurement volume. Moreover, the ability to use virtual detection volumes in the post processing which is more flexible and also offers the opportunity to discard self-products was discussed and applied. The results from a test measurement have been compared to literature and showed good agreement. This successfully proved the applicability of the new system. For the future, one extended measurement volume with sideward detection and several detection volumes is planned which should improve the resolution and allow slot sizes down to 10 microm. Moreover, parallel signal processing should be possible while keeping the advantages already mentioned. Furthermore, dual-burst algorithms shall be implemented as well in order to evaluate burst signals with a low interarrival time which were unterrepresented at the present measurements.

The funding of DFG (CZ55/20-1) is gratefully acknowledged.

REFERENCES

- Absil, L. H. J., Steenbergen, W., Passchier, D. M., 1990, "Time and spatial correlation measurements in the turbulent wake of a circular cylinder using Laser Doppler Anemometry", *Appl. Sci. Res.*, Vol. 47, pp. 247-271.
- Albrecht, H.-E., Borys, M., Damaschke, N., Tropea, C., 2003, "Laser Doppler and Phase Doppler Measurement Techniques", Berlin: Springer-Verlag
- Bayer, C., Shirai, K., Büttner, L., Czarske, J., 2008,

"Measurement of acceleration and multiple velocity components using a laser Doppler velocity profile sensor", *Meas. Sci. Technol.*, Vol. 19, pp. 055401.1-055401.11.

Belmabrouk, H., Michard, M., 1998, "Taylor length scale measurement by laser Doppler velocimetry", *Exp. in Fluids*, Vol. 25, pp. 69-76.

Czarske, J., Büttner, L., Razik, T., Müller, H., 2002, "Boundary layer velocity measurements by a laser Doppler profile sensor with micrometre spatial resolution", *Meas. Sci. Technol.*, Vol. 13, pp. 1979-1989.

Fraser, R., Pack, C. J., Santavicca, D. A., 1986, "An LDV system for turbulence length scale measurements", *Exp. Fluids*, Vol. 4, pp. 150-152.

Nobach, H., Müller, E., Tropea, C., 1998 "Efficient estimation of power spectral density from laser Doppler anemometer data", *Exp. in Fluids*, Vol. 24, pp. 499-509.

Nobach, H., 1999, "Processing of stochastic sampled data in laser Doppler anemometry", *Proceedings, 3rd International Workshop on Sampling theory and applications*, pp. 149-154.

Nobach, H., 2002, "Local time estimation for the slotted correlation function of randomly sampled LDA data", *Exp. Fluids*, Vol. 32, pp. 337-345.

Pope, S.B., 2000, "Turbulent Flows", Cambridge: Cambridge University Press.

Shirai, K., Pfister, T., Büttner, L., Czarske, J., Müller, H., Becker, S., Lienhart, H., Durst, F., 2006, "Highly spatially resolved velocity measurements of a turbulent channel flow by a fiber-optic heterodyne laser-Doppler velocity-profilesensor", *Exp. Fluids*, Vol. 40, pp. 473-481.

Trimis, D. and Melling, A., 1995, "Improved laser Doppler Anemometry techniques for two-point turbulent flow correlations", *Meas. Sci. Technol.*, Vol. 6, pp. 663-673.

van Maanen, H.R.E. and Tummers, M.J., 1996 "Estimation of the auto correlation function of turbulent velocity fluctuations using the slotting technique with local normalization", *Proceedings, 8th International Symposia on Applications of Laser Techniques to Fluid Mechanics, paper 36.4*.